PAPER

# Frequency-Domain MMSE Channel Estimation for Frequency-Domain Equalization of DS-CDMA Signals

**Kazuaki TAKEDA**[†a)], ***Student Member and*** **Fumiyuki ADACHI**[†], ***Member***

**SUMMARY** Frequency-domain equalization (FDE) based on minimum mean square error (MMSE) criterion can replace the conventional rake combining to significantly improve the bit error rate (BER) performance in a frequency-selective fading channel. MMSE-FDE requires an accurate estimate of the channel transfer function and the signal-to-noise power ratio (SNR). Direct application of pilot-assisted channel estimation (CE) degrades the BER performance, since the frequency spectrum of the pilot chip sequence is not constant over the spreading bandwidth. In this paper, we propose a pilot-assisted decision feedback frequency-domain MMSE-CE. The BER performance with the proposed pilot-assisted MMSE-CE in a frequency-selective Rayleigh fading channel is evaluated by computer simulation. It is shown that MMSE-CE always gives a good BER performance irrespective of the choice of the pilot chip sequence and shows a high tracking ability against fading. For a spreading factor *SF* of 16, the $E_b/N_0$ degradation for BER=$10^{-4}$ with MMSE-CE from the ideal CE case is as small as 0.9 dB (including an $E_b/N_0$ loss of 0.28 dB due to the pilot insertion).

***key words:*** *DS-CDMA, frequency-domain equalization, channel estimation, MMSE criterion*

## 1. Introduction

In the 3rd generation (3G) mobile communication systems, wideband direct sequence code division multiple access (DS-CDMA) has been adopted as a wireless access technique for data transmissions of a few Mbps [1]. DS-CDMA can exploit the channel frequency-selectivity by the use of coherent rake combining that resolves the propagation paths having different time delays and coherently combines them to achieve the path diversity gain [2]. Recently, demands for high-speed data transmissions are rapidly increasing even in mobile communication systems and a lot of research attention is paid to the next generation mobile communication systems that support transmission data rates higher than few tens of Mbps [3]. However, for such high-speed data transmissions, the wireless channel is severely frequency-selective [4] and DS-CDMA with rake combining suffers from inter-path interference (IPI) in a severe frequency-selective channel. Therefore, the transmission performance with rake combining significantly degrades when small spreading factor is used (i.e., high data rates for the given chip rate). Hence, the use of some channel equalization techniques instead of rake combining is inevitable for the next mobile communication systems.

It was shown [5]–[7] that the use of simple one-tap frequency-domain equalization (FDE) based on minimum mean square error (MMSE) criterion can replace rake combining while improving the BER performance. Accurate estimation of the channel transfer function and the signal-to-noise power ratio (SNR) are necessary for MMSE-FDE. Numerous studies on channel estimation (CE) are found in [8]–[12]. Pilot-assisted CE is utilized for DS-CDMA with rake combining [3]. However, its direct application to DS-CDMA with MMSE-FDE degrades the BER performance, since the frequency spectrum of the pilot chip sequence is not constant over the spreading bandwidth; thus, the BER performance depends on the choice of the pilot chip sequence. In this paper, we propose a pilot-assisted frequency-domain MMSE-CE for orthogonal multicode DS-CDMA with MMSE-FDE. The performance of the proposed MMSE-CE does not depend on the frequency spectrum of the pilot chip sequence. We evaluate, by computer simulation, its BER performance in a frequency-selective Rayleigh fading channel.

The remainder of this paper is organized as follows. Section 2 presents the transmission system model for the multicode DS-CDMA with MMSE-FDE. In Sect. 3, the proposed frequency-domain decision feedback MMSE-CE is described. Section 4 presents the simulation results for the achievable BER performance in a frequency-selective Rayleigh fading channel. It is shown that the proposed frequency-domain MMSE-CE can always provide a good BER performance irrespective of the choice of the pilot chip sequence. Section 5 gives some conclusions.

## 2. Orthogonal Multicode DS-CDMA with FDE

### 2.1 Overall Transmission System

The transmission system model for the multicode DS-CDMA with MMSE-FDE is illustrated in Fig. 1. At the transmitter, the $u$th code's binary data sequence, $u = 0 \sim (U-1)$, is transformed into a data modulated symbol sequence $\{d^u(n)\}$ and then spread by multiplying it by an orthogonal spreading sequence $c_u(t)$. The resultant $U$ chip sequences are multiplexed and further multiplied by a common scramble sequence $c_{scr}(t)$ to make the resultant multicode DS-CDMA signal white-noise like. Note that an extreme case is the non-spread ($SF$=1) single carrier system. The orthogonal multicode DS-CDMA signal is divided into

Manuscript received July 20, 2006.
Manuscript revised December 28, 2006.
[†]The authors are with the Department of Electrical Communication Engineering, Graduate School of Engineering, Tohoku University, Sendai-shi, 980-8579 Japan.
a) E-mail: takeda@mobile.ecei.tohoku.ac.jp
DOI: 10.1093/ietcom/e90–b.7.1746

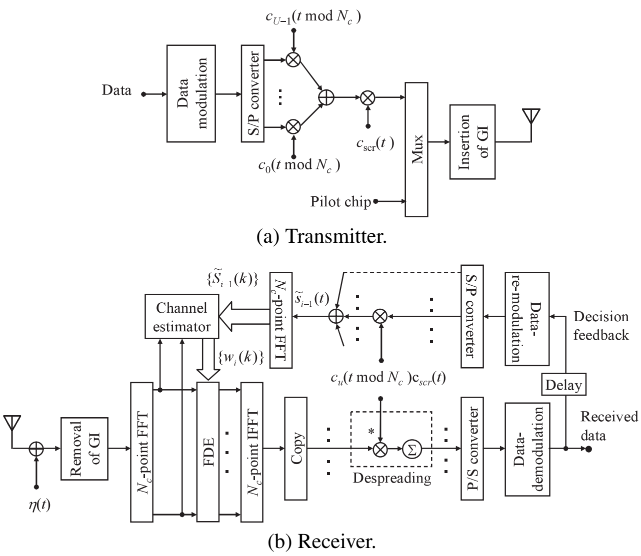


(a) Transmitter.

(b) Receiver.

**Fig. 1** Transmission system model for DS-CDMA with FDE.

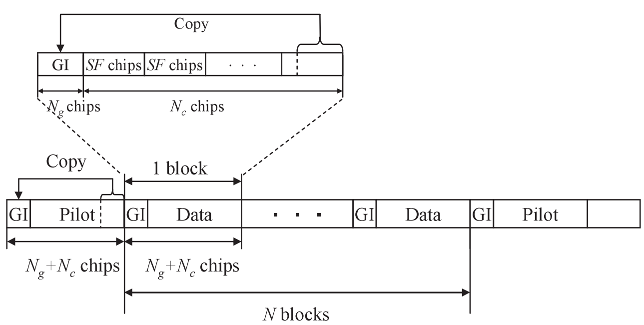


**Fig. 2** Transmit frame structure.

a sequence of blocks of $N_c$ chips each, and the last $N_g$ chips of each block are copied as a cyclic prefix and inserted into the guard interval (GI) placed at the beginning of each block as illustrated in Fig. 2. For pilot-assisted frequency-domain decision feedback MMSE-CE, the pilot chip block is periodically transmitted, each followed by $N$ data chip blocks as shown in Fig. 2.

The GI-inserted chip sequence $\hat{s}(t)$ is transmitted over a frequency-selective fading channel and is received at the receiver. After the removal of the GI, the received chip sequence is decomposed by $N_c$-point FFT into $N_c$ subcarrier components (Note that the terminology "subcarrier" is used for explanation purpose only although subcarrier modulation is not used). After MMSE-FDE, $N_c$-point inverse FFT (IFFT) is applied to obtain the equalized time-domain chip sequence for despreading and data-demodulation.

### 2.2 Frequency-Domain Equalization

Throughout the paper, chip-spaced discrete-time signal representation is used. In the $i$th block, $U$ data symbol sequences $d_i^u(n)$, $u = 0 \sim U-1$ and $n = 0 \sim (N_c/SF - 1)$, are transmitted, where $N_c$ and $SF$ are chosen so that the value of $N_c/SF$ becomes an integer. The $i$th block chip sequence $\hat{s}_i(t)$, $t = -N_g \sim (N_c - 1)$, in one block can be expressed, using the equivalent lowpass representation, as

$$\hat{s}_i(t) = \sqrt{2S}\, s_i\ (t \bmod N_c), \tag{1}$$

where $S$ denotes the transmit power and $s_i(t)$, $t = 0 \sim (N_c - 1)$, is given by

$$s_i(t) = \left[\sum_{u=0}^{U-1} d_i^u\left(\lfloor t/SF \rfloor\right) c_u(t \bmod SF)\right] c_{scr}(t), \tag{2}$$

with $|c_u(t)| = |c_{scr}(t)| = 1$ for $t = 0 \sim (N_c - 1)$, where $\lfloor x \rfloor$ represents the largest integer smaller than or equal to $x$. $i$=0 corresponds to the pilot chip block.

The GI-inserted chip sequence $\hat{s}_i(t)$ is transmitted over a frequency-selective fading channel. At the receiver, after the removal of the GI, the received chip sequence is decomposed by $N_c$-point FFT into $N_c$ subcarrier components $\{R_i(k); k = 0 \sim N_c - 1\}$. Then, MMSE-FDE is carried out to obtain [5]

$$\hat{R}_i(k) = R_i(k) w_i(k), \tag{3}$$

where $w_i(k)$ is the $k$-th subcarrier MMSE equalization weight for the $i$th block, given by [8]

$$w_i(k) = \frac{\bar{H}_i^*(k)}{N_c \left|\bar{H}_i(k)\right|^2 + 2\bar{\sigma}_i^2}, \tag{4}$$

where $\bar{H}_i(k)$ represents the channel gain estimate, $\bar{\sigma}_i^2$ is the noise plus interference power estimate, which will be described in Sect. 3, and * denotes the complex conjugate operation.

$N_c$-point IFFT is applied to transform the frequency-domain signal $\{\hat{R}_i(k); k = 0 \sim N_c - 1\}$ into time-domain chip sequence $\hat{r}_i(t)$, $t = 0 \sim (N_c - 1)$:

$$\hat{r}_i(t) = \frac{1}{N_c} \sum_{k=0}^{N_c-1} \hat{R}_i(k) \exp\left(j2\pi t \frac{k}{N_c}\right). \tag{5}$$

Finally, despreading is carried out on $\hat{r}_i(t)$, giving

$$\hat{d}_i^u(n) = \frac{1}{SF} \sum_{t=nSF}^{(n+1)SF-1} \hat{r}_i(t) c_u^*(t) c_{scr}^*(t), \tag{6}$$

which is the decision variable for data-demodulation, associated with $d_i^u(n)$.

## 3. Decision Feedback Frequency-Domain Channel Estimation

Without loss of generality, we assume unmodulated pilot chip sequence (i.e., $d_0(n) = 1 + j0$ for the pilot chip block). The propagation channel is assumed to be a chip-spaced frequency-selective block fading channel having $L$ discrete paths, each subjected to independent fading. The assumption of block fading means that the path gains remain constant over at least one block duration. The discrete-time channel impulse response $h(\tau)$ can be expressed as [13]

$$h(\tau) = \sum_{l=0}^{L-1} h_l \delta(\tau - \tau_l), \tag{7}$$

where $h_l$ and $\tau_l$ are the complex-valued path gain and the time delay of the $l$th path ($l = 0 \sim L-1$), respectively, with $\sum_{l=0}^{L-1} E[|h_l|^2] = 1$ ($E[.]$ denotes the ensemble average operation).

### 3.1 MMSE-CE Using Pilot Chip Block ($i$=0)

After the removal of the GI, the received pilot chip sequence $r_0(t)$, $t = 0 \sim (N_c - 1)$, can be represented as

$$r_0(t) = \sqrt{2SU} \sum_{l=0}^{L-1} h_l c((t-\tau_l) \bmod N_c) + \eta(t), \tag{8}$$

where $c(t)$ is the pilot chip sequence with $|c(t)| = 1$ and $\eta(t)$ is a zero-mean complex Gaussian process with a variance of $2N_0/T_c$; $N_0$ is the single-sided power spectrum density of the additive white Gaussian noise (AWGN) and $T_c$ is the chip duration. The pilot power is set to $SU$ to keep it the same as the $U$-order code-multiplexed data chip power. The $k$th subcarrier component $R(k)$ of the received pilot chip sequence, obtained by applying $N_c$-point FFT, can be written as

$$R_0(k) = H(k)C(k) + \Pi(k), \tag{9}$$

where $C(k)$, $H(k)$ and $\Pi(k)$ are the $k$th subcarrier component of the pilot chip sequence $c(t)$, the channel gain and the noise component due to the AWGN, respectively. They are given by

$$\begin{cases} C(k) = \sum_{t=0}^{N_c-1} c(t) \exp\left(-j2\pi k \frac{t}{N_c}\right) \\ H(k) = \sqrt{2SU} \sum_{l=0}^{L-1} h_l \exp\left(-j2\pi k \frac{\tau_l}{N_c}\right) \\ \Pi(k) = \sum_{t=0}^{N_c-1} \eta(t) \exp\left(-j2\pi k \frac{t}{N_c}\right) \end{cases}. \tag{10}$$

The noise power per subcarrier is $\sigma^2 = N_c(N_0/T_c)$.

The channel gain $H(k)$ needs to be estimated for MMSE-FDE. For the case of rake combining, $\sqrt{2SU}h_l$ is estimated by taking the time-domain correlation between the received pilot and spreading chip sequence as

$$\hat{h}_l = \frac{1}{N_c} \sum_{t=0}^{N_c-1} r_0(t+\tau_l) c^*(t), \tag{11}$$

which can be rewritten as

$$\hat{h}_l = \frac{1}{N_c} \sum_{k=0}^{N_c-1} \left\{ \frac{1}{N_c} R_0(k) C^*(k) \right\} \exp\left(j2\pi \tau_l \frac{k}{N_c}\right). \tag{12}$$

Since $H(k)$ is the Fourier transform of the channel impulse response $\sqrt{2SU}h(\tau)$, Eq. (12) implies that $\{R_0(k)C^*(k)/N_c\}$ is the estimate $\hat{H}_0(k)$ of $H(k)$. Channel estimation $\hat{H}_0(k) = R_0(k)C^*(k)/N_c$ is matched to the transmitted chip sequence $c(t)$ and can maximize the signal-to-noise power ratio of the estimated channel gain (therefore, this CE is called maximal-ratio combining (MRC)-CE in this paper). $\hat{H}_0(k)$ can be expressed as

$$\hat{H}_0(k) = R_0(k)\mathrm{X}(k), \tag{13}$$

where $\mathrm{X}(k)$ is given by

$$\mathrm{X}(k) = C^*(k)/N_c \quad \text{for MRC-CE.} \tag{14}$$

The division by $N_c$ in Eq. (14) is because of the fact that $E[|C(k)|^2] = N_c$. The frequency spectrum of the pilot chip sequence $c(t)$ is not constant over the spreading bandwidth (i.e., $C(k) \neq$ const.). Therefore, the channel estimation accuracy depends on the pilot chip sequence and the achievable BER performance may degrade since the spectrum nulls in the pilot chip spectrum are sometimes produced.

In this paper, to avoid this problem, we propose an MMSE-CE that minimizes the mean square error (MSE) between $\hat{H}_0(k)$ and $H(k)$. We define the estimation error $e(k)$ as

$$\begin{aligned} e(k) &= \hat{H}_0(k) - H(k) \\ &= H(k)[\mathrm{X}(k)C(k) - 1] + \mathrm{X}(k)\Pi(k). \end{aligned} \tag{15}$$

We want to find $\mathrm{X}(k)$ that minimizes the MSE $E[|e(k)|^2]$ for the given $C(k)$. Since $E[|H(k)|^2] = 2SU$ and $\Pi(k)$ is a zero-mean complex-valued noise having the variance $2\sigma^2$, the MSE for the given $C(k)$ becomes

$$E[|e(k)|^2] = 2SU \begin{bmatrix} 1 + |\mathrm{X}(k)C(k)|^2 - 2\mathrm{Re}[\mathrm{X}(k)C(k)] \\ + \left(\frac{SU}{\sigma^2}\right)^{-1} |\mathrm{X}(k)|^2 \end{bmatrix}. \tag{16}$$

Hence, solving $\partial E[|e(k)|^2]/\partial \mathrm{X}(k) = 0$ gives

$$\mathrm{X}(k) = \frac{C^*(k)}{|C(k)|^2 + \left(\frac{SU}{\sigma^2}\right)^{-1}} \quad \text{for MMSE-CE.} \tag{17}$$

Neglecting the second term in the denominator of Eq. (17) represents the zero forcing (ZF)-CE case:

$$\mathrm{X}(k) = \frac{C^*(k)}{|C(k)|^2} \quad \text{for ZF-CE.} \tag{18}$$

However, with using ZF-CE, the channel estimation accuracy significantly degrades due to the noise enhancement when the spectrum nulls appear in the frequency-domain.

### 3.2 Estimation of Signal-to-Noise Power Ratio

As understood from Eq. (17), MMSE-CE requires the estimation of the signal-to-noise power ratio $SU/\sigma^2$. From Eq. (8), the instantaneous received signal power is given by $SU\sum_{l=0}^{L-1}|h_l|^2$. Since $\sum_{l=0}^{L-1} E[|h_l|^2] = 1$, if $L$ is large (i.e., strong frequency-selective channel), then we have

$$SU \sum_{l=0}^{L-1} |h_l|^2 \approx SU \tag{19}$$

due to the law of large numbers [2]. Therefore $SU\sum_{l=0}^{L-1}|h_l|^2$ can be an unbiased estimator of $SU$.

The ZF-CE is performed to get the tentative channel estimate $\hat{H}_{ZF}(k)$ using Eqs. (13) and (18). $N_c$-point IFFT is applied to $\{\hat{H}_{ZF}(k);\ k=0\sim(N_c-1)\}$ to obtain the instantaneous channel impulse response $\hat{h}_{ZF}(\tau)$. Since the actual channel impulse response $h(\tau)$ is assumed to be present only within the GI length and $\hat{h}_{ZF}(\tau)$ is the estimate of $\sqrt{2SU}h_l$, the average signal power $SU$ can be estimated, from Eq. (19), as

$$\hat{S}_0=\frac{1}{2}\sum_{\tau=0}^{N_g-1}|\hat{h}_{ZF}(\tau)|^2. \tag{20}$$

On the other hand, the noise due to the AWGN is uniformly distributed over an entire range (i.e., $\tau=0\sim N_c-1$). Assuming that all the impulse response beyond the GI is composed of the noise component only, the noise power $\sigma^2$ can be estimated as

$$\hat{\sigma}_0^2=\frac{1}{2}\frac{N_c}{N_c-N_g}\sum_{\tau=N_g}^{N_c-1}|\hat{h}_{ZF}(\tau)|^2. \tag{21}$$

Hence, X($k$) for MMSE-CE in Eq. (17) can be replaced, using (20) and (21), by

$$\mathrm{X}(k)=\frac{C^*(k)}{|C(k)|^2+\left(\dfrac{\hat{S}_0}{\hat{\sigma}_0^2}\right)^{-1}}\quad\text{for MMSE-CE}. \tag{22}$$

### 3.3 Delay Time-Domain Windowing & Decision Feedback ($i=1\sim N$)

The channel estimate is perturbed by the noise due to the AWGN. In this paper, the delay time-domain windowing technique [9] and the decision feedback [10] are introduced to reduce the noise effect. Figure 3 shows the channel estimation block diagram using delay time-domain windowing and decision feedback.

In the decision feedback, the $(i-1)$th block decision $\hat{d}_{i-1}^u(n)$, $u=0\sim U-1$, is fedback as a pilot for the MMSE-CE and FDE operations at the $i$th block, $i=1\sim N$. Respreading of $\hat{d}_{i-1}^u(n)$ and $U$-order code-multiplexing are performed to generate the replica $\tilde{s}_{i-1}(t)$ of the $(i-1)$th block chip sequence. $N_c$-point FFT is applied to decompose $\tilde{s}_{i-1}(t)$ into $N_c$ subcarrier components. The $k$-th subcarrier component $\tilde{S}_{i-1}(k)$ is obtained as

$$\tilde{S}_{i-1}(k)=\sum_{t=0}^{N_c-1}\tilde{s}_{i-1}(t)\exp\left(-j2\pi k\frac{t}{N_c}\right). \tag{23}$$

Replacing $C(k)$ in Eq. (22) by $\tilde{S}_{i-1}(k)/\sqrt{U}$ as a pilot, MMSE-CE is carried out to get $\hat{H}_{i-1}(k)$ of the $(i-1)$th block corresponding to Eq. (13) (the division of $\tilde{S}_{i-1}(k)$ by $\sqrt{U}$ comes from the relationship between $E[|\tilde{S}_{i-1}(k)|^2]=UN_c$ and $E[|C(k)|^2]=N_c$). $\hat{H}_{i-1}(k)$ is transformed by applying $N_c$-point IFFT into the instantaneous channel impulse response $\hat{h}_{i-1}(\tau)$, $\tau=0\sim N_c-1$. $\hat{h}_{i-1}(\tau)$ can be obtained as

$$\hat{h}_{i-1}(\tau)=\frac{1}{N_c}\sum_{k=0}^{N_c-1}\hat{H}_{i-1}(k)\exp\left(j2\pi\tau\frac{k}{N_c}\right). \tag{24}$$

By replacing $\hat{h}_{i-1}(\tau)$ with zeros for $\tau\geq N_g$ and applying $N_c$-point FFT, the improved estimate $\tilde{H}_{i-1}(k)$ is obtained since the noise power reduces by $N_g/N_c$ times. $\tilde{H}_{i-1}(k)$ is obtained as

$$\tilde{H}_{i-1}(k)=\sum_{\tau=0}^{N_g-1}\hat{h}_{i-1}(\tau)\exp\left(-j2\pi k\frac{\tau}{N_c}\right). \tag{25}$$

To suppress the error propagation due to the decision error in the previous block, the first order filtering with forgetting factor $\alpha$ is applied [11]. The channel gain estimate $\bar{H}_i(k)$ for the $i$th block is given by

$$\bar{H}_i(k)=\begin{cases}\tilde{H}_0(k), & i=0\\ (1-\alpha)\bar{H}_{i-1}(k)+\alpha\tilde{H}_{i-1}(k), & i=1\sim N\end{cases}, \tag{26}$$

where the $i$=0th block is the pilot block and $\tilde{H}_0(k)$ is obtained by the pilot block only. When the practical channel estimation is used, $\bar{\sigma}_i^2$ in Eq. (4) should be the contribution

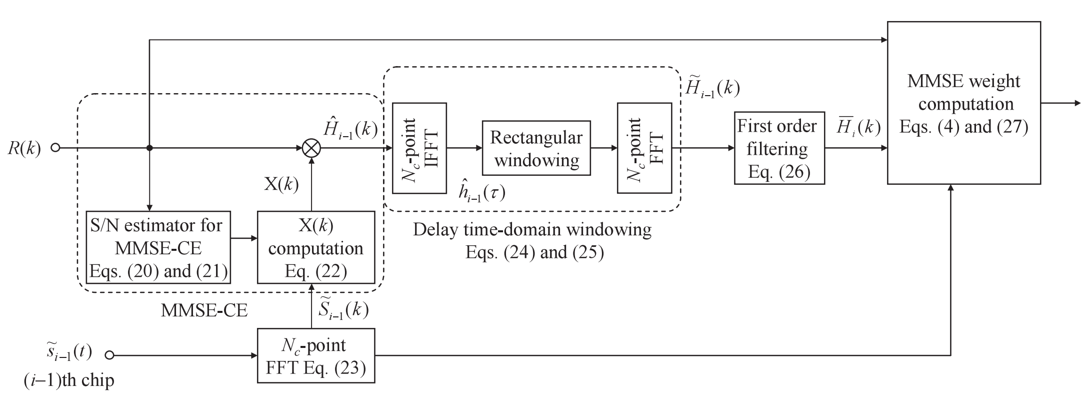


**Fig. 3** MMSE-CE using delay time-windowing and decision feedback.

from both the AWGN and the channel estimation error. $\bar{\sigma}_i^2$ is obtained as

$$\bar{\sigma}_i^2 = \frac{1}{2}\frac{1}{N_c}\sum_{k=0}^{N_c-1}\left|R_{i-1}(k) - \bar{H}_i(k)\left(\frac{1}{\sqrt{U}}\tilde{S}_{i-1}(k)\right)\right|^2. \quad (27)$$

When MMSE-CE is used, the expectation of $\bar{H}_i(k)$ is not the same as the exact value of $H_i(k)$ (i.e., $E[\bar{H}_i(k)] \neq H_i(k)$). Hence, the direct substitution of $\bar{H}_i(k)$ into (27) produces a biased noise estimate $\bar{\sigma}_i^2$ for MMSE-CE. To obtain an unbiased noise estimate $\bar{\sigma}_i^2$, $\bar{H}_i(k)$ is divided by the following coefficient $A_i$:

$$A_i = \begin{cases} \dfrac{1}{N_c}\displaystyle\sum_{k=0}^{N_c-1}\dfrac{|C(k)|^2}{|C(k)|^2+\left(\dfrac{\hat{S}_0}{\hat{\sigma}_0^2}\right)^{-1}} & \text{for } i=0 \\ (1-\alpha)A_{i-1}+\alpha\left\{\dfrac{1}{N_c}\displaystyle\sum_{k=0}^{N_c-1}\dfrac{\frac{1}{U}\left|\tilde{S}_{i-1}(k)\right|^2}{\frac{1}{U}\left|\tilde{S}_{i-1}(k)\right|^2+\left(\dfrac{\hat{S}_0}{\hat{\sigma}_0^2}\right)^{-1}}\right\} & \\ \quad \text{for } i=1\sim N & \end{cases}. \quad (28)$$

For the derivation of Eq. (28), we have used Eq. (26) and

$$E\left[\tilde{H}_i(k)\right] = \begin{cases} \dfrac{1}{N_c}\displaystyle\sum_{k'=0}^{N_c-1}\dfrac{|C(k')|^2}{\frac{1}{U}|C(k')|^2+\left(\dfrac{\hat{S}_0}{\hat{\sigma}_0^2}\right)^{-1}}H(k) & \\ \quad \text{for } i=0 & \\ \dfrac{1}{N_c}\displaystyle\sum_{k'=0}^{N_c-1}\dfrac{\frac{1}{U}\left|\tilde{S}_i(k')\right|^2}{\frac{1}{U}\left|\tilde{S}_i(k')\right|^2+\left(\dfrac{\hat{S}_0}{\hat{\sigma}_0^2}\right)^{-1}}H(k) & \\ \quad \text{for } i=1\sim N & \end{cases}, \quad (29)$$

which has been obtained from Eqs. (13), (22)–(25). The expectation of $\bar{H}_i(k)/A_i$ becomes $H_i(k)$ and hence, substituting $\bar{H}_i(k)/A_i$ into Eq. (27) gives the unbiased noise estimate $\bar{\sigma}_i^2$ for MMSE-CE.

## 4. Computer Simulation

The simulation parameters are summarized in Table 1. Quaternary phase shift keying (QPSK) data modulation, $N_c$=256, $N_g$=32, and an $L$-path frequency-selective Rayleigh fading channel having uniform power delay profile are assumed. We assume that the time delay $\tau_l$ of the $l$th ($l = 0 \sim L-1$) path is $l$ chips. Ideal sampling timing is assumed at the receiver. One frame consists of 16 chip blocks; one pilot chip block is followed by 15 data chip blocks ($N$=15). The repetition of an M-sequence of 255 chips or 4095 chips is used as the pilot chip sequence $c(t)$. The SNR estimation technique described in Sect. 3 is used.

**Table 1** Simulation parameters.

| | | |
|---|---|---|
| Transmitter | Modulation | QPSK |
| | Number of FFT points | $N_c$=256 |
| | GI | $N_g$=32 (chips) |
| | Spreading sequence | Product of Walsh sequence and PN sequence |
| | Pilot chip sequence | M-sequence with a repetition of 255, 4095 chips |
| | Spreading factor | $SF$=1,16 |
| Channel | Fading | Frequency-selective Rayleigh fading |
| | Power delay profile | $L$-path uniform power delay profile |
| | Number of paths | $L$=1~32 |
| Receiver | Frequency-domain equalization | MMSE |

### 4.1 Comparison of MMSE-, ZF- and MRC-CE

The BER performances of DS-CDMA with MMSE-FDE using MMSE-, MRC- and ZF-CE are plotted in Fig. 4 as a function of the average received bit energy-to-AWGN power spectrum density ratio $E_b/N_0$, defined as $E_b/N_0 = 0.5SF(1+N_g/N_c)(E_c/N_0)(16/15)$ ($E_c/N_0$ is the average received chip energy-to-AWGN spectrum density ratio), for $SF$=$U$=1 and 16. An $L$=16-path block Rayleigh fading and a normalized maximum Doppler frequency of $f_D(N_c+N_g)T_c = 0.001$ are assumed (this corresponds to a terminal moving speed of 75km/h for a chip rate of 100 Mcps and 5 GHz carrier frequency). We have found, by computer simulation, the first order filter forgetting factor $\alpha$ that gives the minimum BER at $E_b/N_0$=15 dB; $\alpha$ is set as $\alpha$=0.2 for MMSE-CE, $\alpha$=0.1 for MRC-CE, and $\alpha$=0 for ZF-CE. For comparison, the BER performance with ideal CE is also plotted. MMSE-CE gives the best performance irrespective of the pilot chip sequence pattern since the noise enhancement can be avoided. However, when a 4095-chip pilot sequence is used, MRC- and ZF-CE significantly degrade the BER performance compared to the use of a 255-chip pilot sequence. This is due to larger variations in the pilot chip spectrum for 4095-chip sequence than for 255-chip sequence. ZF-CE provides the worst performance. This is because when the frequency component $C(k)$ of pilot chip sequence is zero at some frequencies, the channel estimate becomes infinite and this produces BER floor (With MMSE-CE, the channel estimate never becomes infinity due to the presence of the second term $(SU/\sigma^2)^{-1}$ in the denominator of Eq. (17)). When $SF$=1 and 16, the $E_b/N_0$ degradation from the ideal CE is as small as 0.9 dB with MMSE-CE (about 0.28 dB is due to the pilot insertion). It can be concluded that, when MMSE-CE is used, the channel estimation accuracy is almost insensitive to the choice of the pilot chip sequence. We have also confirmed, by our simulation, that the perfor-

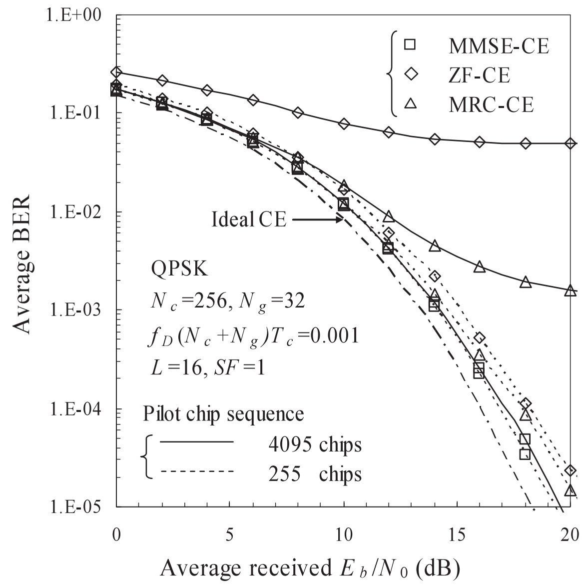


(a) $SF$=1.

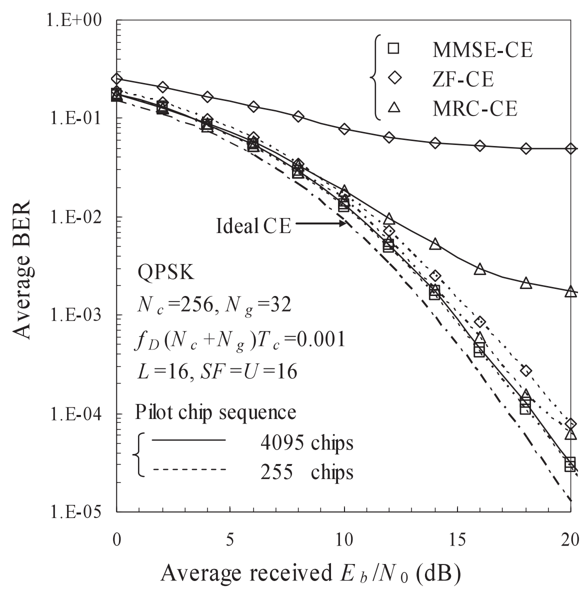


(b) $SF=U$=16.

**Fig. 4** Comparison of MMSE-, ZF-, and MRC-CE.

mance of MMSE-FDE using MMSE-CE is not so sensitive to the accuracy of SNR estimation.

## 4.2 Impact of the Number of Paths

The BER performance of MMSE-CE is plotted in Fig. 5 as a function of the number $L$ of paths at the average received $E_b/N_0$=10 and 20 dB, when $SF=U$=16 and $f_D(N_c+N_g)T_c$ = 0.001. For comparison, the BER performance with ideal CE is also plotted. As $L$ increases, the BER performance improves since larger frequency diversity gain is obtained by MMSE-FDE. It is understood from Fig. 5 that the performance degradation from the ideal CE case is almost the same irrespective of $L$.

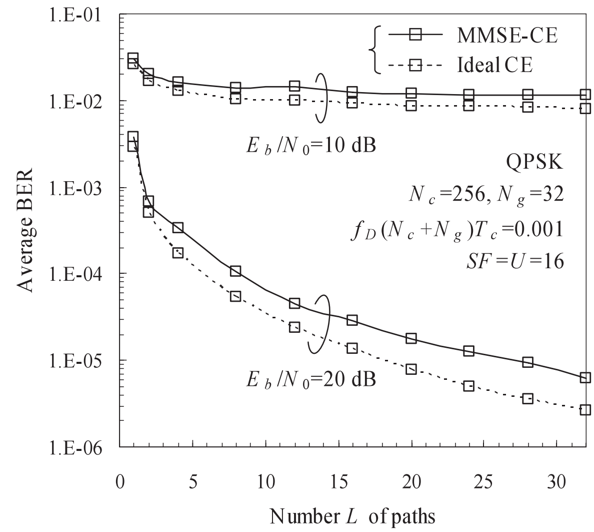


**Fig. 5** Impact of the number $L$ of paths on BER performance.

## 4.3 Impact of Fading Rate

The pilot block is sent every $N+1$ block and hence the tracking ability against fading is lost for fast fading. Although, so far, we have assumed block fading, if the fading becomes too fast and the channel gains vary in a chip block, the subcarrier components of the transmitted DS-CDMA signal can not be properly extracted by FFT. It is interesting to see the impact of $f_D$ on the BER performance. The BER dependency on the fading rate is plotted as a function of the normalized maximum Doppler frequency $f_D(N_c+N_g)T_c$ for MMSE- and MRC-CE in Fig. 6 when the average $E_b/N_0$=15 dB and $SF=U$=1 (Fig. 6(a)) and 16 (Fig. 6(b)). M-sequence of a repetition of 255 chips is assumed as the pilot sequence. MMSE-CE always gives better BER performance than MRC-CE. The BER is almost constant when $f_D(N_c+N_g)T_c \le 0.002$; however, the BER starts to increase when $f_D(N_c+N_g)T_c$ increases beyond 0.004 since the tracking ability against fading starts to deteriorate. Furthermore, the BER significantly degrades when $f_D(N_c+N_g)T_c \ge 0.01$. This is because the channel gain varies within a block of $N_c$ chips and hence, proper FFT cannot be done.

Figure 7 shows the average BER performances using MMSE- and MRC-CE as a function of the average received $E_b/N_0$ for $f_D(N_c+N_g)T_c$ = 0.001 and 0.01. For $f_D(N_c+N_g)T_c$ = 0.01, the first order filter forgetting factor is $\alpha$=0.7 for MMSE-CE and $\alpha$=0.4 for MRC-CE. When $f_D(N_c+N_g)T_c$ = 0.01, the BER floor is seen; in the case of $SF$=1, a BER floor of around $1\times10^{-3}$ is produced with MRC-CE, while the BER floor is reduced to $1\times10^{-5}$ with MMSE-CE. For the case of $SF$=16, a BER floor of around $1\times10^{-3}$ is seen with MRC-CE, while the BER floor is reduced to $6\times10^{-5}$ with MMSE-CE. The reason why the BER floor of $SF$=16 is higher than that of $SF$=1 is that the residual inter-chip interference produced by imperfect channel

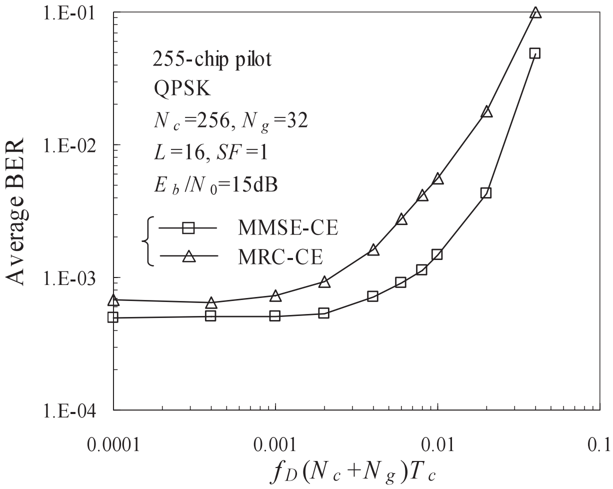


(a) $SF$=1.

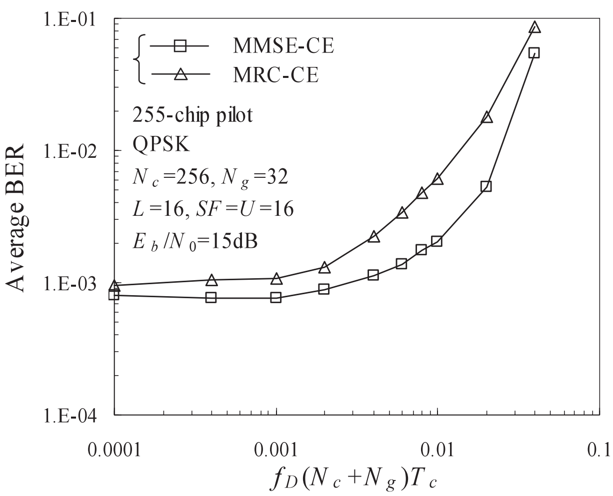


(b) $SF$=$U$=16.

**Fig. 6** BER dependency on fading rate.

estimation distorts the orthogonality among the codes.

## 5. Conclusion

In this paper, we proposed pilot-assisted decision feedback frequency-domain MMSE-CE for DS-CDMA with MMSE-FDE. Decision feedback and first order filtering were introduced in MMSE-CE to further improve the estimation accuracy. The achievable BER performance in a frequency-selective Rayleigh fading channel was evaluated by computer simulation. ZF- and MRC-CE degrade the BER performance since the pilot frequency spectrum is not constant over the spreading bandwidth. However, it was shown that the achievable BER performance with MMSE-CE is almost insensitive to the choice of the pilot chip sequence and that MMSE-CE always provides better BER performance and higher tracking ability against time-varying channel than ZF- and MRC-CE.

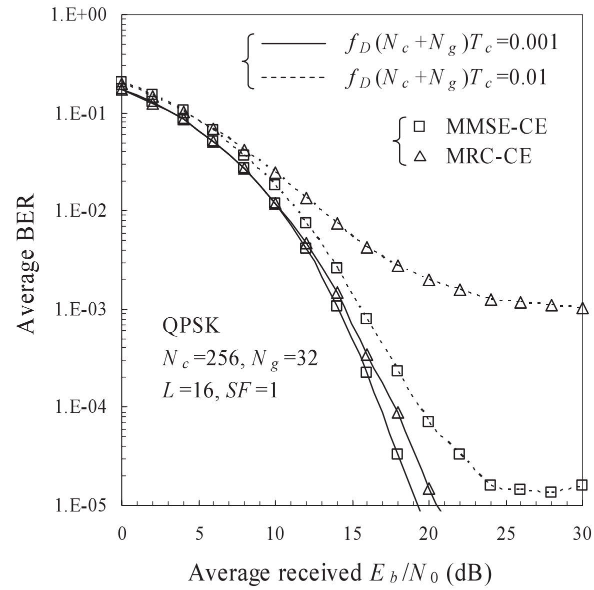


(a) $SF$=1.

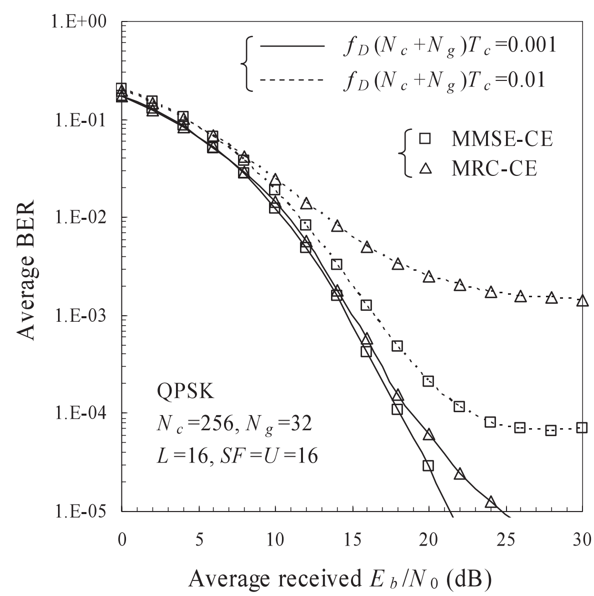


(b) $SF$=$U$=16.

**Fig. 7** Impact of fading rate on BER performance.

### References

[1] F. Adachi, M. Sawahashi, and H. Suda, "Wideband DS-CDMA for next generation mobile communications systems," IEEE Commun. Mag., vol.36, pp.56–69, Sept. 1998.
[2] J.G. Proakis, Digital communications, 3rd ed., McGraw-Hill, 1995.
[3] Y. Kim, et al., "Beyond 3G: Vision, requirments, and enabling technologies," IEEE Commun. Mag., vol.41, pp.120–124, March 2003.
[4] W.C. Jakes, Jr., ed., Microwave mobile communications, Wiley, New York, 1974.
[5] F. Adachi, D. Garg, S. Takaoka, and K. Takeda, "Broadband CDMA techniques," IEEE Wireless Commun. Mag., vol.12, no.2, pp.8–18, April 2005.
[6] F.W. Vook, T.A. Thomas, and K.L. Baum, "Cyclic-prefix CDMA with antenna diversity," Proc. IEEE VTC 2002 Spring, pp.1002–1006, May 2002.

[7] I. Martoyo, G.M.A. Sessler, J. Luber, and F.K. Jondral, "Comparing equalizers and multiuser detections for DS-CDMA downlink systems," Proc. IEEE VTC 2004 Spring, pp.1649–1653, May 2004.
[8] J.-J. van de Beek, O. Edfors, M. Sandell, S.K. Wilson, and P.O. Borjesson, "On channel estimation in OFDM systems," Proc. 45th IEEE Veh. Technol. Conf., pp.815–819, Chicago, IL, July 1995.
[9] T. Fukuhara, H. Yuan, Y. Takeuchi, and H. Kobayashi, "A novel channel estimation method for OFDM transmission technique under fast time-variant fading channel," Proc. 57th IEE Veh. Technol. Conf., pp.2343–2347, Jeju, Korea, April 2003.
[10] K. Ishihara, K. Takeda, and F. Adachi, "Decision feedback channel estimation for OFDM with STTD," Proc. 7th International Symposium on Wireless Personal Multimedia Communications (WPMC), pp.V3-455–V3-459, Abano Terme, Italy, Sept. 2004.
[11] S. Takaoka and F. Adachi, "Frequency-domain channel estimation using FFT/IFFT for DS-CDMA mobile radio," Proc. 60th IEEE Veh. Technol. Conf. (VTC), vol.1, pp.694–698, Los Angeles, CA, Sept. 2004.
[12] P. Hoeher, S. Kaiser, and P. Robertson, "Pilot-symbol-aided channel estimation in time and frequency," Proc. Global Telecomm. Conf. the Mini-conf., pp.90–96, Nov. 1997.
[13] T.S. Rappaport, Wireless communications, Prentic Hall, 1996.

**Kazuaki Takeda** received his B.E., M.S. and Dr. Eng. degrees in communications engineering from Tohoku University, Sendai, Japan, in 2003, 2004 and 2007 respectively. Currently he is a postdoctoral fellow at the Department of Electrical and Communications Engineering, Graduate School of Engineering, Tohoku University. Since 2005, he has been a Japan Society for the Promotion of Science (JSPS) research fellow. His research interests include equalization, interference cancellation, transmit/receive diversity, and multiple access techniques. He was a recipient of the 2003 IEICE RCS (Radio Communication Systems) Active Research Award and 2004 Inose Scientific Encouragement Prize.

**Fumiyuki Adachi** received the B.S. and Dr. Eng. degrees in electrical engineering from Tohoku University, Sendai, Japan, in 1973 and 1984, respectively. In April 1973, he joined the Electrical Communications Laboratories of Nippon Telegraph & Telephone Corporation (now NTT) and conducted various types of research related to digital cellular mobile communications. From July 1992 to December 1999, he was with NTT Mobile Communications Network, Inc. (now NTT DoCoMo, Inc.), where he led a research group on wideband/broadband CDMA wireless access for IMT-2000 and beyond. Since January 2000, he has been with Tohoku University, Sendai, Japan, where he is a Professor of Electrical and Communication Engineering at the Graduate School of Engineering. His research interests are in CDMA wireless access techniques, equalization, transmit/receive antenna diversity, MIMO, adaptive transmission, and channel coding, with particular application to broadband wireless communications systems. From October 1984 to September 1985, he was a United Kingdom SERC Visiting Research Fellow in the Department of Electrical Engineering and Electronics at Liverpool University. Dr. Adachi served as a Guest Editor of IEEE JSAC on Broadband Wireless Techniques, October 1999, Wideband CDMA I, August 2000, Wideband CDMA II, Jan. 2001, and Next Generation CDMA Technologies, Jan. 2006. He is an IEEE Fellow and was a co-recipient of the IEEE Vehicular Technology Transactions Best Paper of the Year Award 1980 and again 1990 and also a recipient of Avant Garde award 2000. He was a recipient of IEICE Achievement Award 2002 and a co-recipient of the IEICE Transactions Best Paper of the Year Award 1996 and again 1998. He was a recipient of Thomson Scientific Research Front Award 2004.